Chapter 5: Towards Photoswitchable Chemotherapy Agents

In this chapter, the design and synthesis of two new photoswitchable chemotherapy agents is reported. The photochemical properties of these switches are studied using UV-vis and NMR spectroscopy. An outlook on further research is presented at the end of the chapter.

5.1 General introduction

Chemotherapy was first utilized in the early 20th century and has become a life-saving standard in the treatment of cancer.[1] However, the cytotoxicity of chemotherapeutic agents is non-specific, since any type of fast dividing cell in the body is targeted.[2] Therefore, side effects of chemotherapy can be severe and discontinuation of treatment in seriously ill patients is often preferred over the heavy discomfort induced by it. In fact, a recent survey among doctors revealed that most would choose to stop high intensity treatment in the last months of their own life.[3] The side effects arising from chemotherapeutic agents may be battled if drug activity can be controlled externally at a precisely defined location. Among several potential triggers, light stands out due to its non-invasive nature and the high level of spatial and temporal control over the application.[4]

Photopharmacology is a relatively new field which aims at using light to control activity of therapeutic agents. Contrary to photocaging, in photopharmacology the drug can not only be switched "on" at the desired location, but can also be switched "off".[5] In photopharmacology, a photoswitch is synthetically incorporated in the structure of an existing drug. The ideal photopharmacological drug is inactive when in the thermodynamically stable form, due to the photoswitch distorting the structure. Upon irradiation, the drug switches to an active form which fits the receptor because the structure is similar to that of the parent drug. Inactivation by either irradiation or a thermal process ensures that the active form of the drug is not excreted. A variety of switches including azobenzenes,[6] stilbenes[7] and spiropyrans[8] have been used in the design of photopharmacological drugs. However, the use of multistate switches has not yet been reported. Thus far, a variety of photoswitchable drugs has been successfully synthesized and tested. A comprehensive overview, as well as an outlook on current challenges and future developments, can be found in references 9-13.

5.2 Photoswitchable cisplatin derivatives

(*Cis*-Diamminedichloro)platinum(II) (cisplatin) is a widely used chemotherapy agent that is particularly effective in the treatment of prostate cancer.[14] Although the compound was already described in 1844,[15] it's anticancer activity was not discovered until the late 1960's.[16] In the cell, cisplatin undergoes double ligand exchange to form $Pt[(OH_2)_2(NH_2)_2]$.[14] Subsequently, the platinum binds to purine bases in DNA and thus creates interstrand and intrastrand crosslinks. These crosslinks distort the helical structure, ultimately leading to cell apoptosis. Conversely, (*trans*-diamminedichloro)platinum(II) (transplatin) is much less effective at inducing crosslinks,[17,18] but at higher concentration it is able to inhibit replication.[19]

Recently, Presa *et al.* presented two photoswitchable platinum complexes (Scheme 5.1).[20] The core structure of compound **DAE-Pt** is a diarylethene photoswitch functionalized with pyridine moieties, which act as ligands in a Pt(II) complex. A difference in cytotoxicity against various cell lines was observed, with the closed form of **DAE-Pt** being more toxic. The authors explain this difference by considering that the planar structure of the closed switch may be more efficient at intercalation, allowing the platinum to bind to the purine bases.

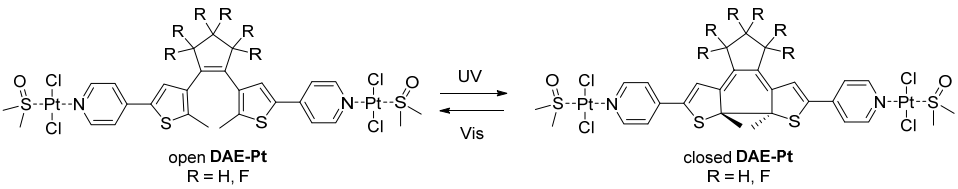

Scheme 5.1: Structure and switching behaviour of diarylethene based platinum(II) complex **DAE-Pt**.

5.2.1 Design and synthesis

Platinum complexes induce cell apoptosis through crosslinking of the DNA strands (*vide supra*). Although the work of Presa *et al*. constitutes an interesting proof of principle regarding the application of photopharmacology to platinum-based chemotherapy agents, the actual differences in activity between the open and closed form of the switch are small.[20] As an alternative, we considered using an overcrowded-alkene based multistate molecular photoswitch (molecular motor) to control the crosslinking process. A molecular motor has two thermally stable forms, *cis* and *trans*. In this paragraph, these are denominated *Z* and *E*, respectively, to avoid confusion with the different coordination around the Pt (II) square planar complex. In the *Z* isomer (Figure 5.1b, right), the substituents on two halves of a first generation molecular motor are positioned relatively close to each other while in the *E* isomer they are spatially distant (Figure 5.1b, left). This allows the substituents to work in concert in the *Z* isomer, a concept which has successfully been applied to perform asymmetric catalysis.[21] We believe that using the large displacement of substituents upon irradiation may attribute to a larger difference in activity. Our design features a *trans* platinum complex attached to each half of the motor. The *E* isomer of this compound is expected to be comparable in activity to transplatin (Figure 5.1a, left and 1b, left). Photoswitching the motor from *E* to *Z* forms might induce binding of both Pt complexed to the DNA, forming a type of crosslink, analogous to the complex activity of cisplatin (Figure 5.1a, right, and 1b, right.). In doing so, we change from a traditional mononuclear complex, such as cisplatin, to a bisnuclear complex. Additionally, the change in chirality between the unstable *Z* and stable *Z* isomers could attribute to a difference in complexation efficiency, providing a first multistate photopharmacological agent.

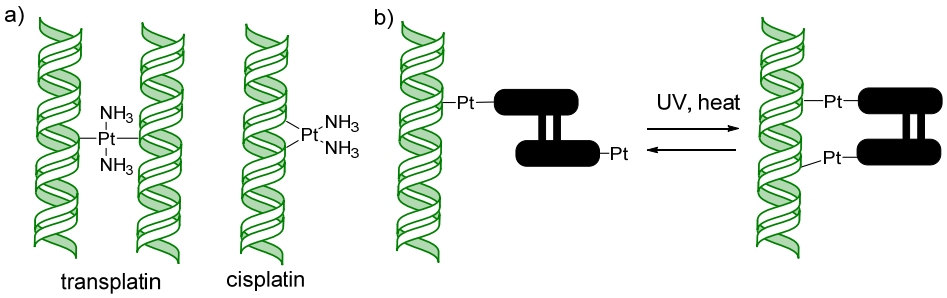

Figure 5.1: Schematic overview of (a) the mode of operation of transplatin and cisplatin and (b) a molecular motor based platinum complex for use in DNA crosslinking studies.

Structure **5.2** (Scheme 5.2) was proposed as the photoswitchable, cytotoxic Pt(II) complex. A first generation molecular motor functionalized with pyridine moieties (**5.1**) was selected as the photoswitchable ligand, analogous to the functionalized diarylethene ligand that was used by Presa *et al.*[20] The synthesis started from dibromo-substituted compound *Z*-**2.7**, which is easily accessed through four high yielding synthetic steps (see Chapter 2). The pyridine moieties were installed *via* a Suzuki cross-coupling and ligand *Z*-**5.1** was obtained in 32% yield. Complexation to the platinum yielded complexed motor *Z*-**5.2**.

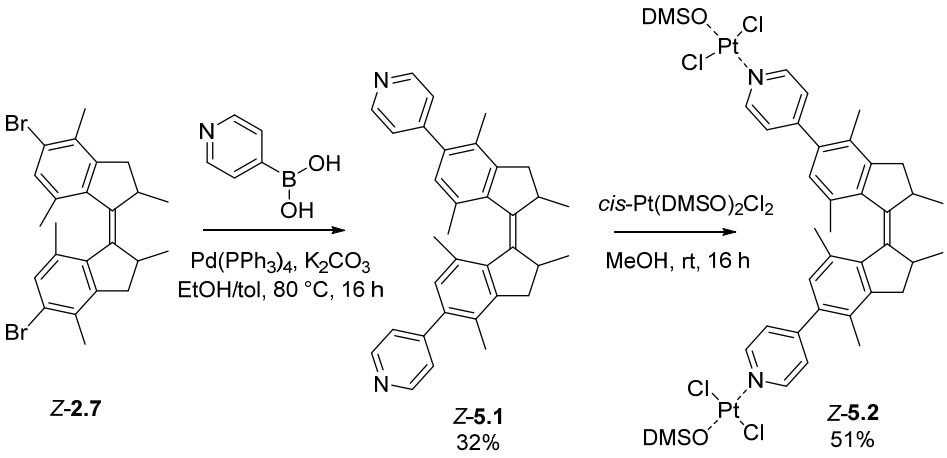

Scheme 5.2: Synthesis of Pt(II) based motor **5.2**. Configuration around the platinum in **5.2** has not been confirmed.

Complexation of the platinum could be observed in ^{1}H NMR by a shift of the characteristic two doublets corresponding to the pyridine moieties of the motor unit, and was confirmed using HRMS. Notably, while *cis*-Pt(DMSO)$_2$Cl$_2$ was used for complexation, the *trans* complex was expected to be the product.[20,22] Although the configuration around the platinum was not confirmed for **5.2**, *cis-trans* isomerization during the complexation reaction was found for the analogous diarylethene Pt complex.[20] This isomerization can be attributed to the S-bonded DMSO ligand exhibiting the strongest *trans* effect.[22]

5.2.2 NMR analysis of rotary cycle

^{1}H NMR analysis was used to study the rotational cycle of Pt-complexed motor **5.2** (Figure 5.2). A solution of stable *Z*-**5.2** in CD_2Cl_2 was irradiated with λ = 365 nm light. The half-life of the unstable *E* isomer of xylene-based first generation molecular motors, such as **5.2**, is typically very short (<1 min at rt). Therefore, upon photogenerated isomerization, thermal helix inversion (THI) of the unstable *E* isomer towards the stable *E* isomer can occur readily even at low temperatures (Figure 5.2a). This stable *E* isomer can also undergo photoisomerization, thus creating a mixture of all four isomers. To prevent THI of the unstable *E* isomer, all irradiation and measurements were performed at -50 °C. Despite these precautions, after 2 h of irradiation of *Z*-**5.2** (Figure 5.2ii) the sample contained not only 71% of the unstable *E* isomer, but also 14% of the stable *E* isomer and even 6% of the unstable *Z* isomer, which emerged as a result of photochemical isomerization from stable *E*. After heating the sample to room temperature for 30 min, all of the formed unstable *E* isomer is converted to the stable *E* isomer (Figure 5.2iii). The percentage of unstable *Z* isomer in this spectrum remains unchanged, which is to be expected since the unstable *Z* isomer of xylene-based first generation molecular motors typically has a half-life of several days at room temperature. For the second half of the cycle, the sample was irradiated for 10 h with λ = 365 nm light (Figure 5.2iv), leading to a PSS consisting of 93% unstable *Z* isomer. Finally, the stable *Z* isomer was regenerated by heating the sample to 35 °C for 6 h (Figure 5.2v). Overall, motor **5.2** appears to have excellent photochemical properties in CD_2Cl_2, with high conversions during the photochemical isomerizations and no significant degradation observed.

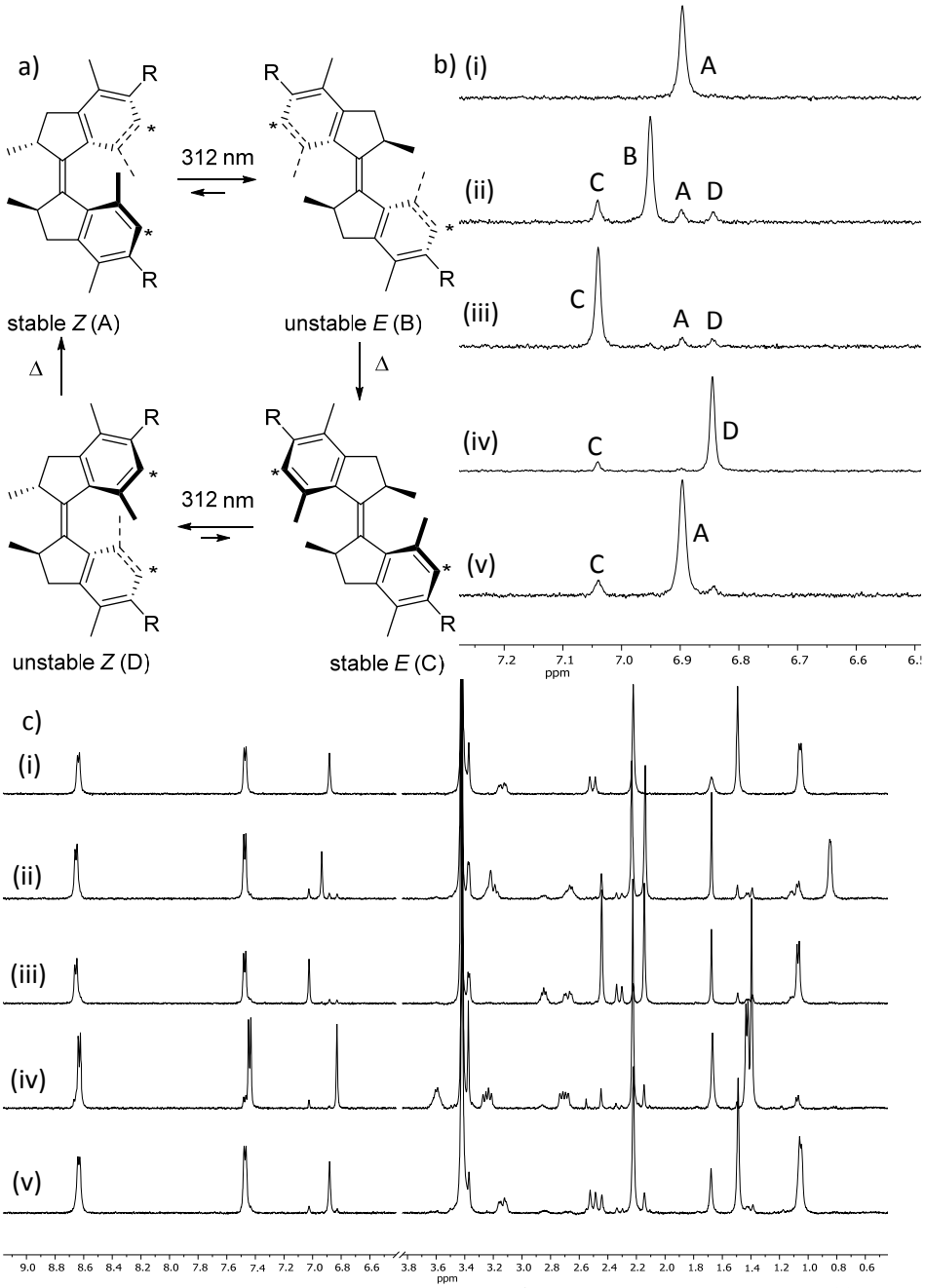

Figure 5.2: Photochemical and thermal rotary cycle of cisplatin derivative motor **5.2**. (a) Rotary cycle of simplified structure of motor **5.2** (R = pyridine-Pt[Cl_2DMSO]). (b) ^{1}H NMR analysis of switching cycle, zoomed in on H*. Isomers are indicated by letters A-D, see (a) for assignment. (i) Stable *Z*, (ii) λ = 365 nm,-50 °C, 2 h, (iii) rt, 30 min, (iv) λ = 365 nm, -50 °C, 10 h, (v) 35 °C, 6 h. All spectra recorded in CD_2Cl_2 at -50 °C. (c) ^{1}H NMR analysis of rotary cycle, full spectra.

5.2.3 DNA-binding assay

In order to test the effect of Pt(II) complexed motor **5.2** the compound was incubated with pBR322 plasmid DNA.[23] Typically, when plasmid DNA is incubated with cisplatin complexes, the DNA is shortened which results in a longer migration rate in gel electrophoresis.[18] No such effect was observed for plasmid DNA incubated with motor **5.2**. Most likely, this is due to insufficient solubility of **5.2** in the assay medium. Even in buffer solutions containing up to 10% DMSO, motor **5.2** remained completely insoluble. The presence of DMSO is highly discouraged in studies concerning cisplatin derivatives, since DMSO can lead to loss of cytotoxicity.[24] Therefore, the use of higher percentages of DMSO was deemed unsuitable. The addition of water-solubilizing groups, such as demonstrated in Chapter 4, may provide a solution to this problem.

5.3 Photoswitchable colchicine derivatives

Colchicine (Scheme 5.3) is a natural product isolated from *Colchicum autumnale*, a type of crocus, which has found limited application as an anti-cancer agent.[25] It acts as a microtubule inhibitor, blocking the polymerization of tubulin. Combretastatin-4A (Scheme 5.3) is a member of a large group of natural products isolated from *Combretum caffum*, and acts as a very potent inhibitor of the colchicine binding domain in the protein.[26–28] Notably, combretastatin-4A has a stilbenoid core and can potentially be switched between its *cis* and *trans* isomers using light. The *trans* isomer was found to be much less active.[27,29] Recently, three groups separately reported on the development of **azo-C4A** (Scheme 5.3), a derivative of combretastatin 4A in which the bridging olefinic bond were replaced by a diazo moiety, thus forming an azobenzene structure.[30–32] *Cis*-**azo-C4A** was found to have excellent cytotoxic abilities and is 250 times more potent than the *trans* isomer. *In vivo* experiments were used to show that control over microtubulin growth could be achieved using light, as well as a high cytotoxity in a variety of cell lines. However, it was also demonstrated that **azo-C4A** is easily reduced in the presence of glutathione. Glutathione is a reducing agent that is present in the cell in millimolar concentrations.[33] Azobenzene can be reduced to hydrazobenzene or the free amine, both of which are carcinogenic.[34] Resistance against glutathione reduction can be improved by changing substituents,[35] but this may be impractical for combretastatin-4A derivatives since both phenyl rings are involved in binding.[25]

Combretastatin-4A does not suffer from such side effects. However, no photoswitching experiments have been performed, most likely since stilbenes tend to undergo irreversible photocyclization in the planar *cis* isomer.[36] This issue can be resolved by demobilizing the free rotation around the vinyl-phenyl bonds by installing five-membered rings on each half. The resulting stiff-stilbenes are not susceptible to photocyclization.[37] With this in mind, we proposed stiff-stilbene *cis*-**5.3** (Scheme 5.3) as an alternative photoswitchable colchicine analogue. We expect this compound to be resistant to glutathi-

one reduction. Additionally, both isomers of stiff-stilbenes are thermally stable whereas **azo-C4A** readily undergoes thermal *cis-trans* isomerization.

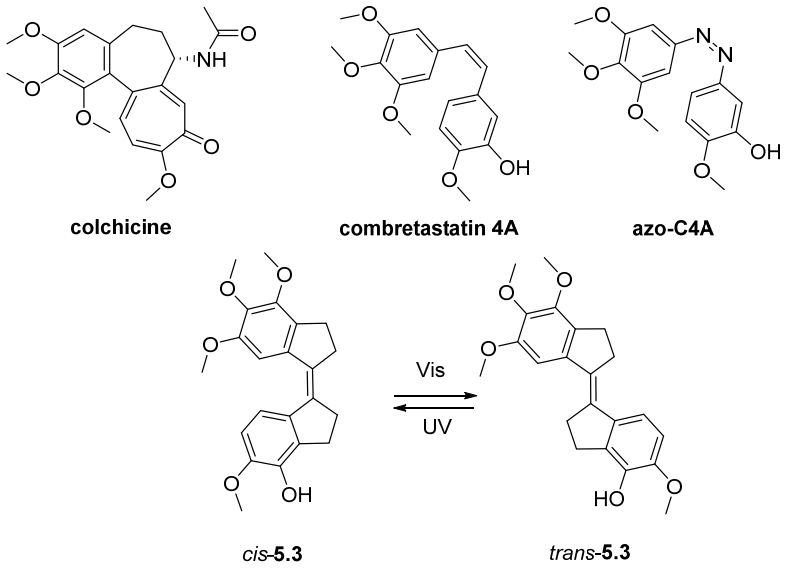

Scheme 5.3: Structures of the natural products colchicine and combretastatin-4A, azobenzene derivative **azo-C4A** and proposed switchable colchicine-domain inhibitor **5.3** with its switching cycle.

5.3.1 Synthesis

Scheme 5.4 shows the synthesis of colchicine derivative **5.3**. Indanone **5.4** was synthesized according to literature procedure, *via* a triflic anhydride-mediated Vilsmeyer-Haack type reaction of 1,2,3-trimethoxybenzene and dimethylacrylamide.[38] Although only 22% yield was obtained, this reaction could be performed on a large scale and was therefore deemed preferable to the alternative three step synthetic route analogous to the synthesis of indanone **5.7** (*vide infra*). The synthesis towards the other half of the target compound started with a Knoevenagel reaction between 2,3-dimethoxybenzaldehyde and malonic acid. Styryl carboxylic acid **5.5** was obtained in 82% yield and subsequently reduced in quantitative yield using palladium on carbon and hydrogen gas. Cyclization of the resulting compound **5.6** towards indanone **5.7** using polyphosphoric acid proceeded with poor (8%) yield. Conversion of **5.8** into the corresponding acyl chloride using $SOCl_2$ and subsequent cyclization through an $AlCl_3$-mediated Friedel-Crafts acylation was more successful, and indanone **5.7** was obtained in 65% yield. Selective deprotection of one methoxy substituent was achieved by following a literature procedure,[39] using a chloroaluminate ionic liquid reagent. Indanone **5.8** was obtained in 69% yield, as a 6/1 mixture of regioisomers, from which the preferred regioisomer could be obtained through recrystallization (55% overall yield).

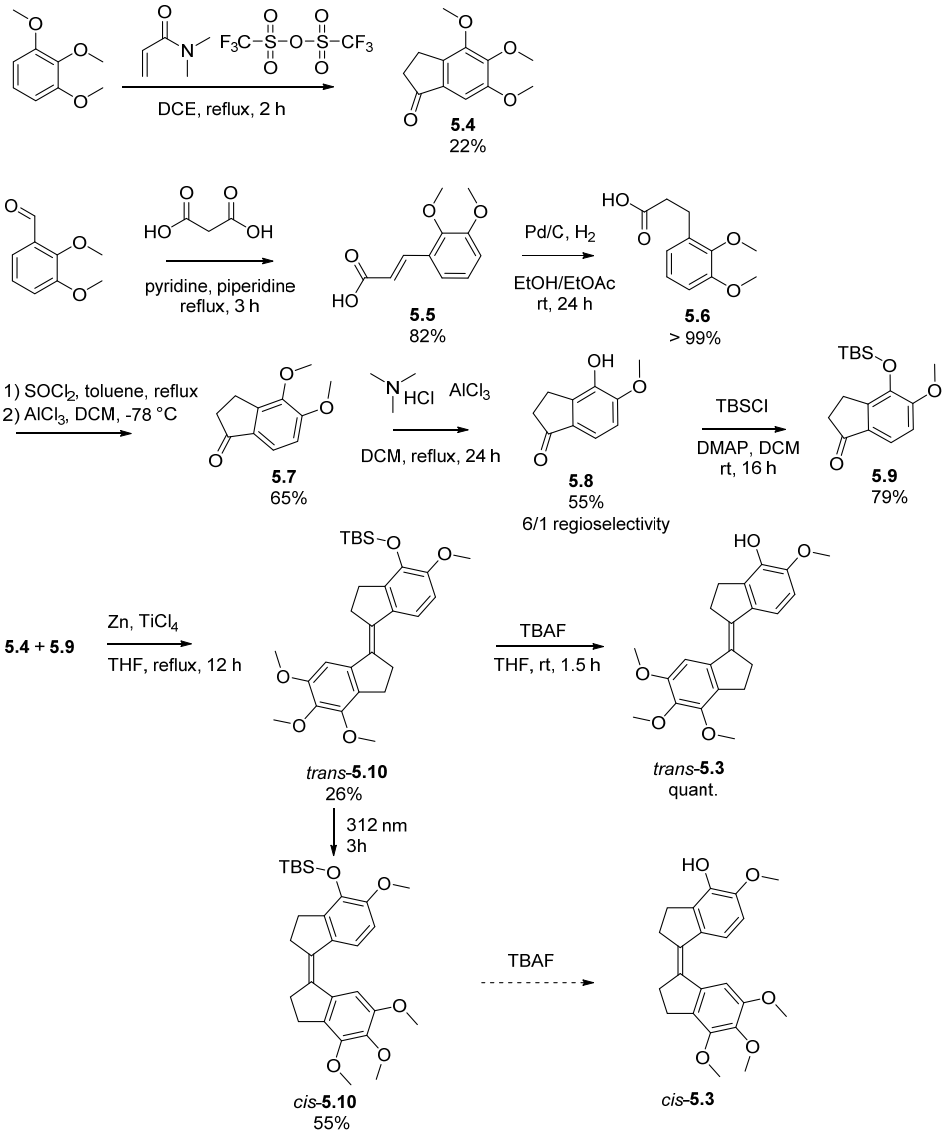

Scheme 5.4: Synthesis of colchicine derivative **5.3**.

The newly deprotected phenol was protected with a *tert*-butyl dimethylsilyl group in 79% yield. Protected colchicine derivative **5.10** was synthesized *via* a mixed McMurry reaction between indanones **5.4** and **5.9**. Although homocoupling was also observed, the product could be isolated in 26% yield through column chromatography. Due to steric hindrance, only one isomer of **5.3** was formed, which was determined to be *trans* by NOE spectroscopy (Figure 5.3). The crosslinks between the aromatic region (H_A, H_B and H_c) and the aliphatic region (all four methoxy peaks, and the cyclopentane peaks) are depicted. In the *trans* isomer, cross peaks between the aromatic protons and the

cyclopentane protons on the other half of the switch are seen. In the *cis* isomer, only cross peaks between the aromatic protons and the adjacent methoxy protons are observed. Finally, the TBS group was cleaved using tetrabutyl ammonium fluoride and colchicine derivative *trans*-**5.3** was obtained in quantitative yield.

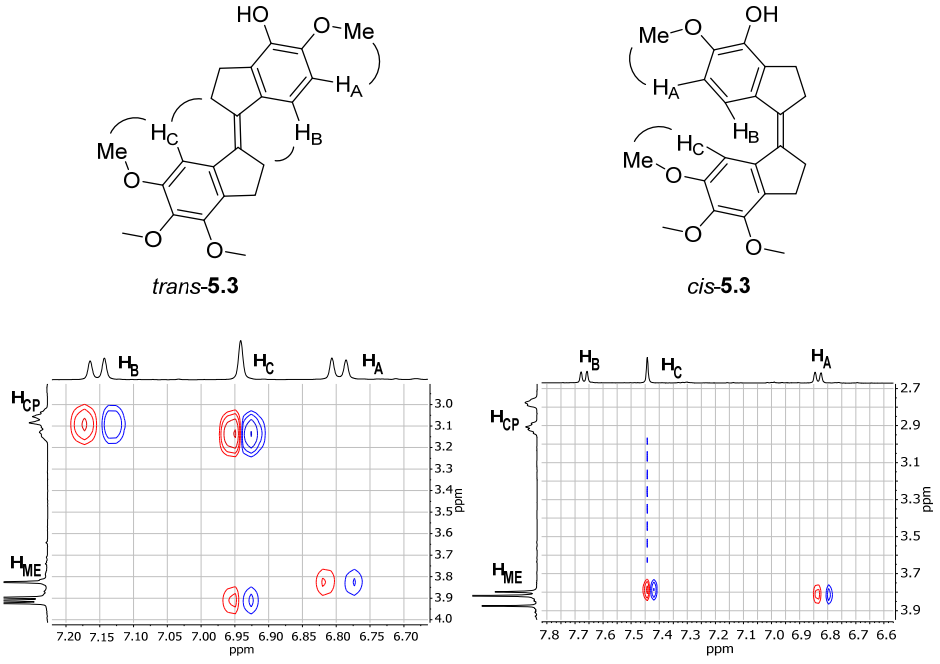

Figure 5.3: NOE spectra of both isomers of **5.3** (part of spectrum). The left spectrum was obtained from the reaction product, the right spectrum from the product after irradiation. Spectra show NOE interaction between the aromatic (X axis) and aliphatic (Y axis) parts of the molecule. Cross-peaks between the protons on the five membered rings (broad multiplet, H_{CP}) and the aromatic protons H_B and H_C indicate that the product obtained from the McMurry reaction is the *trans* isomer (NOE interactions indicated in structure). In the spectrum on the right these cross peaks are absent, which is expected for the *cis* isomer. Both spectra shows cross-peaks between H_A and its neighbouring methoxy group, and H_C and its neighbouring methoxy group.

Colchicine analogue *trans*-**5.3** proved to be a sensitive compound, degrading both under air and acidic conditions. In order to obtain larger quantities of the suspected active compound *cis*-**5.3**, a sample of its precursor *cis*-**5.10** was irradiated with λ = 312 nm light in acetonitrile under an argon atmosphere. After 3 hours, a PSS consisting of 55% *cis* isomer was reached. The isomers of **5.10** could subsequently be separated using column chromatography. Deprotection of *trans*-**5.10** to *trans*-**5.3** appeared successful by TLC and crude NMR analysis. However, after column chromatography no product could be obtained. Stiff-stilbene *cis*-**5.3** is likely to be equally unstable as the *trans* isomer, which in combination with the small scale may have caused the failure of this isolation.

5.3.2 UV-vis analysis

The photochemical behaviour of stiff-stilbene *trans*-**5.3** was analysed using UV-vis spectroscopy. A solution of *trans*-**5.3** in DMSO was purged with argon and a UV-vis spectrum was recorded (Figure 5.4a, black line). The spectrum showed absorption bands with maxima at λ = 322, 336 and 354 nm. The sample was irradiated with 312 nm light and spectra were recorded at regular intervals. The absorption bands decreased in intensity and a new shoulder around 370 nm appeared. Initially, a clear isosbestic point indicated the absence of unwanted side reactions, but after 18 min of irradiation a shift in the isosbestic point at λ = 360 nm was observed and the irradiation was halted. Subsequently, the PSS mixture (Figure 5.4b, black line) was irradiated with blue light (λ = 400 nm) (Figure 5.4b, dashed lines). The new higher wavelength shoulder disappeared while the double absorption band of the *trans* isomer increased. The spectrum at PSS is very similar to that of *trans*-**5.3** (Figure 5.4a, black line), albeit with a lower absorbance at both λ_{max}. To test the stability of the switch, a sample of *trans*-**5.3** in DMSO was irradiated with alternating 312 nm and 400 nm light, for 20 minutes each. The fatigue graph (Figure 5.4b, insert) shows the absorbance of the sample at 353 nm after each irradiation with 312 nm light (white bands) and 400 nm light (grey bands). From this graph it is evident that the switch is highly sensitive to photoinduced degradation. As a control, a solution of **5.3** and a solution of **5.3** that was irradiated for 20 min at λ = 312 nm were monitored over several hours at room temperature. In these solutions, no degradation was observed, supporting the hypothesis that the photogenerated intermediates are unstable, and not *trans*-**5.3** or *cis*-**5.3**. Photoisomerization of **5.3** was also attempted in DCM, which led to almost instant degradation.

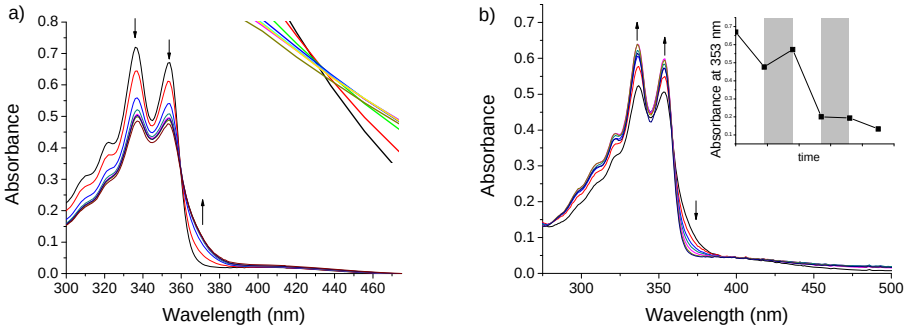

Figure 5.4: UV-Vis analysis of *trans*-**5.3** in DMSO. (a) *Trans*-**5.3** (black line), irradiated with 312 nm light (coloured lines). Insert shows a close-up of the isosbestic point. (b) PSS mixture from (a), irradiated with 400 nm light. The insert shows the absorbance at 353 after continuous irradiation with alternatively 312 light (white bands) and 400 nm light (grey bands). All samples recorded and irradiated at 20 °C.

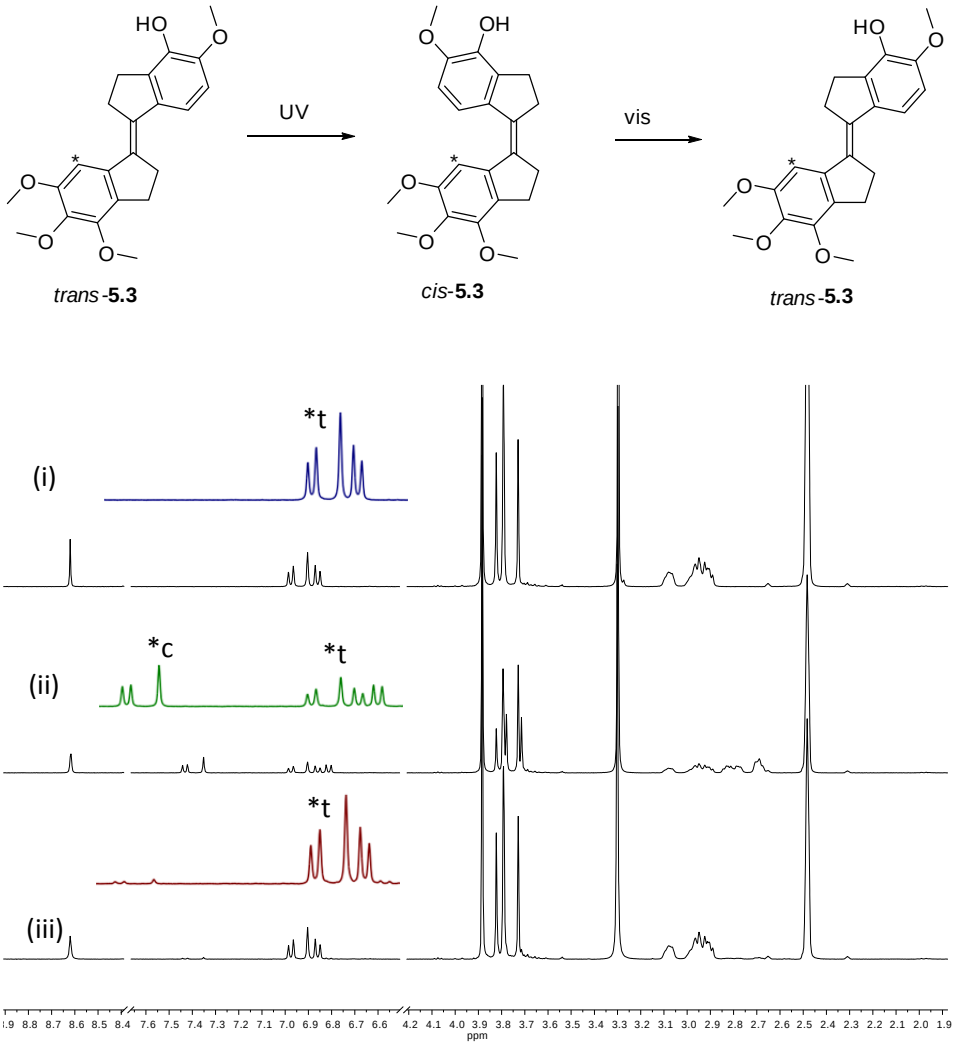

Figure 5.5: Switching cycle of *trans*-**5.3** (top) and ^{1}H NMR analysis of irradiation of colchicine derivative *trans*-**5.3** (bottom). Inserts show zoomed in region between 6.8 and 7.5 ppm. (i) *Trans*-**5.3**. (ii) PSS mixture achieved after irradiation with 312 nm light for 3 h. (iii) PSS mixture achieved after irradiation with 400 nm light for 2h. All spectra were recorded in DMSO-d6 at 20 °C. Proton * (singlet) is marked in the spectra for both the *trans* (*t) and *cis* (*c) isomers.

5.3.3 NMR analysis

The switching process of **5.3** was analysed using ^{1}H NMR spectroscopy. *Trans*-**5.3** was dissolved in DMSO-d6 under an argon atmosphere (Figure 5.5i). After 3 h of irradiation, the PSS was reached, consisting of 55% *cis*-**5.3** and 45% *trans*-**5.3** (Figure 5.5ii). Irradiation of the PSS mixture with blue light (400 nm) leads to an almost complete reformation of *trans*-**5.3** (*trans*/*cis* 96/4, Figure 5.5iii). An internal standard was added to the sample (dichloroethane, δ = 3.88) to monitor stability. No significant degradation was observed. The difference in stability between the NMR sample and the UV-vis sample (*vide supra*) is most likely due to the concentration. Although in both cases the sample was degassed carefully, trace amounts of oxygen may have induced noticeable degradation in the UV-vis sample.

5.3.4 Glutathione reduction

As discussed previously, glutathione reduction of **azo-C4A** to toxic aniline derivatives can be problematic for future *in vivo* applications. The parent Combretastatin A-4 does not suffer from this side reaction.[32] We subjected colchicine analogue **5.3** to a glutathione reduction assay. A 20 µM solution of **5.3** was prepared in a 10 mM glutathione solution of 7.5% DMSO in PBS buffer (pH = 7.4). The absorption at 350 nm was monitored over time (Figure 5.6, black line). An initial 30 min period of rapid degradation was followed by a long period of slow degradation. As a control, the same solution was prepared without the presence of glutathione (Figure 5.6, red line). Although the initial decrease in absorption was slower, after 1 h this sample had degraded as much as the sample containing glutathione, and the absorption continued decreasing at a similar rate. We therefore decided to monitor the stability of **5.3** in a solution containing much less buffer. 20% PBS buffer was required to dissolve the glutathione. The absorbance of the sample with (Figure 5.6, blue line) and without (turquoise line) glutathione was monitored over time in a 4/1 DMSO/PBS buffer mixture. Both samples remain stable for over 4 h. Obviously the glutathione reduction may be compromised by the high concentration of DMSO. However, based on the data shown in Figure 5.6, degradation in the presence of water seems more likely.

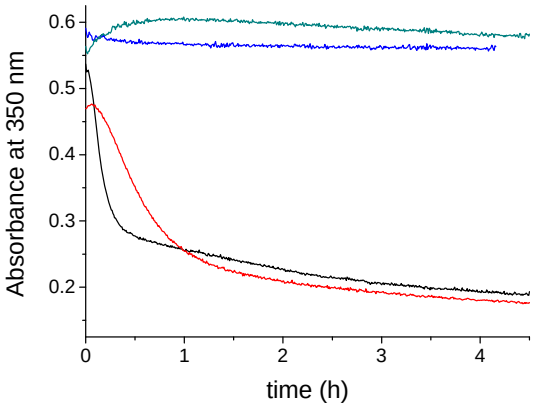

Figure 5.6: Absorption of solution of **5.3** monitored over time. 7.5% DMSO in PBS buffer (pH = 7.4), 10 mM glutathione (black line), 7.5% DMSO in PBS buffer (pH = 7.4), no glutathione (red line), 80% DMSO in PBS buffer (pH = 7.4), 10 mM glutathione (blue line) and 7.5% DMSO in PBS buffer (pH = 7.4), no glutathione (turquoise line).

5.3.5 Water solubility

Both **azo-C4A** and our new colchicine derivative **5.3** are insoluble in water. Borowiak *et al.* addressed this issue by functionalizing **azo-c4A** with a disodium phosphate group (Scheme 5.5).[30] The synthetic procedure used to convert **azo-C4A** into **azo-PC4A** can easily be adapted to install a solubilizing group on **5.3**. Scheme 5.5 depicts the proposed synthesis of water soluble prodrug **5.12**. Initially, the free phenol is converted into dibenzylphosphate **5.11**, after which the disodium salt **5.12** can be obtained by successive treatment with TMSI and sodium methoxide. Due to the instability of **5.3**, not enough material was available to proceed with this synthesis.

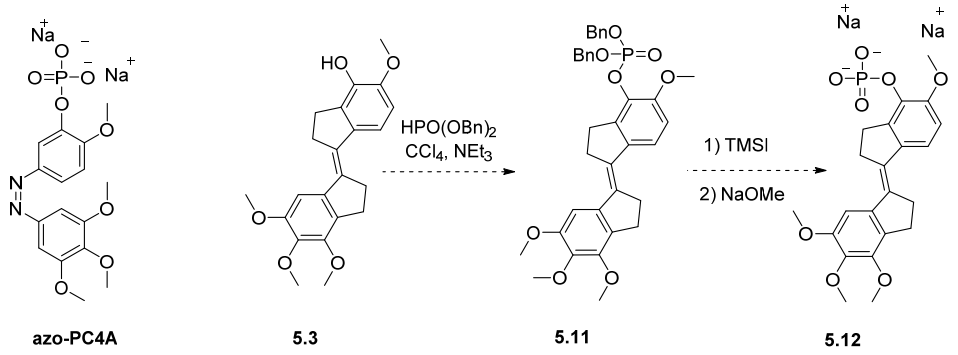

Scheme 5.5: Structure of water soluble prodrug **azo-PC4A**, and proposed synthesis for water soluble prodrug **5.12**.

5.4 Conclusions and outlook

Two potential photoswitchable chemotherapy agents have been synthesized and analysed. First generation Pt complexed motor **5.2** was designed as a cisplatin analogue, modelled after a previously reported diarylethene-based design.[20] NMR studies revealed that the motor has excellent photochemical properties, i.e. high photostationary states and stability in DCM. Due to the lack of solubility in water, the cytotoxicity of motor **5.2** could not be tested. A redesign of the motor is required to continue the investigation. At the time this research was conducted, a stable water soluble motor had not yet been developed and the project was paused. However, taking into account our recent development of water soluble motors (Chapter 3), we currently hold all the tools necessary to take on such a challenge.

Stiff-stilbene **5.3** was designed as a more robust analogue of azobenzene-based combretastatin-A4 derivatives. The *trans* isomer only absorbs in the UV range, but the (active) *cis* isomer can be switched almost quantitatively with blue light. Although compound **5.3** was prone to decomposition under irradiation, the addition of a water-solubilizing group may as an added benefit protect the free phenol, which may be prone to light-induced oxidation. Preliminary investigations indicate that our design is more resistant to glutathione reduction than the related azobenzene **azo-c4A**, but prone to water induced degradation. Again, the addition of a solubilizing group on the vulnerable phenol position may change the stability of **5.3**, and further investigations should be performed on proposed water soluble colchicine derivative **5.12**. Cytotoxicity assays will be performed to see whether **5.3** has the large difference in activity between isomers that is typical of combretastatin-A4 and its derivatives.

5.5 Experimental procedures and acknowledgements

For General Remarks, see Chapter 2. The cytotoxicity assays for platinum-complexed motor *cis*-**5.2** were performed by Daniel Devlitsarov under the guidance of Mickel Hansen.

4,4'-(2,2',4,4',7,7'-hexamethyl-2,2',3,3'-tetrahydro-[1,1'-biindenylidene]-5,5'-diyl)dipyridine (5.1)

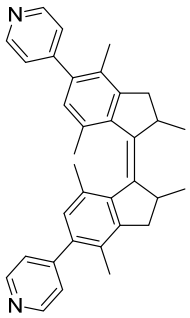

Compound *Z*-**2.7** (100 mg, 0.211 mmol), pyridine-4-boronic acid (104 mg, 0.844 mmol), $Pd(PPh_3)_4$ (37 mg, 0.032 mmol) and K_2CO_3 (146 mg, 1.06 mmol) were mixed in 15 mL of a 3/1 ethanol/toluene mixture and the solution was heated to 80 ºC. The reaction mixture was stirred at 80 °C for 16 h and subsequently quenched with brine (15 mL). The aqueous layer was extracted with ethyl acetate (3 x 10 mL). The combined organic layers were dried over $MgSO_4$ and concentrated *in vacuo*. The crude product was first purified by flash column chromatography (SiO_2, pentane/ethyl acetate 2/3) and sub-

sequently recrystallized from hot ethyl acetate. Motor *Z*-**5.1** was obtained as a yellow solid (32 mg, 0.068 mmol, 32%). ^{1}H NMR (400 MHz, $CDCl_3$) δ 8.64 – 8.58 (m, 4H), 7.28 (d, *J* = 5.0 Hz, 4H), 6.83 (s, 2H), 3.41 (app. p, 2H), 3.16 (dd, *J* = 15.1, 6.3 Hz, 2H), 2.51 (d, *J* = 15.0 Hz, 2H), 2.19 (s, 6H), 1.58 (s, 6H), 1.13 (d, *J* = 6.7 Hz, 6H); ^{13}C NMR (101 MHz, $CDCl_3$) δ 150.4, 149.6, 145.9, 141.3, 141.3, 138.0, 133.5, 129.6, 127.9, 124.8, 77.4, 42.0, 39.6, 20.9, 20.8, 16.8; mp = 296 °C; HRMS (ESIpos): calcd for ($[C_{34}H_{34}N_2 + H]^+$) 471.27948, found 471.27877.

(Pt[Cl_2DMSO)])$_2$-4,4'-(2,2',4,4',7,7'-hexamethyl-2,2',3,3'-tetrahydro-[1,1'-biindenylidene]-5,5'-diyl)dipyridine (5.2)

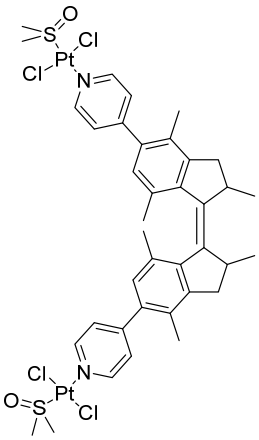

trans-Dichlorobis(dimethyl sulfoxide)platinum(II) (58 mg, 0.14 mmol) was suspended in methanol (12 mL) and heated at reflux until the complex had completely been dissolved. The hot reaction mixture was filtered over a cotton plug into a Schlenk flask containing motor **5.1** (32 mg, 0.068 mmol) under a nitrogen atmosphere. The flask was closed with a rubber septum and the reaction mixture was stirred at room temperature. After 16 h, the reaction mixture was filtered over a glass filter and washed with cold methanol. The motor *Z*-**5.2** was obtained as a yellow solid (40 mg, 0.035 mmol, 51%). ^{1}H NMR (400 MHz, $CDCl_3$) δ 8.71 (d, *J* = 6.4 Hz, 4H), 7.41 (d, *J* = 6.4 Hz, 4H), 6.82 (s, 2H), 3.48 (s, 12H), 3.42 (app. p, 2H), 3.15 (dd, *J* = 15.2, 6.3 Hz, 2H), 2.51 (d, *J* = 15.1 Hz, 2H), 2.20 (s, 6H), 1.54 (s, 6H), 1.11 (d, *J* = 6.6 Hz, 6H); ^{13}C NMR (101 MHz, $CDCl_3$) δ 154.2, 151.3, 146.5, 142.4, 141.8, 135.9, 133.9, 129.8, 128.1, 126.3, 77.4, 44.5, 42.0, 39.6, 20.9, 20.7, 16.6; mp: degrades > 280 °C; HRMS (ESIpos): calcd for ($[C_{38}H_{48}Cl_4N_2O_2Pt_2S_2 + H]^+$) 1159.11507, found 1159.11062.

4,5,6-trimethoxy-2,3-dihydro-1H-inden-1-one (5.4)

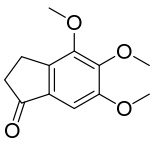

N,N-dimethylacrylamide (5.90 g, 59.5 mmol, 6.13 mL) was dissolved in 105 mL anhydrous dichloroethane and cooled to 0 ºC under a nitrogen atmosphere. Over a period of 10 min, a solution of triflic anhydride (16.8 g, 59.5 mmol, 10.0 mL) in 70 mL of anhydrous dichloroethane was added dropwise. Subsequently, 1,2,3-trimethoxybenzene (10.0 g, 59.5 mmol) dissolved in 70 mL of anhydrous dichloroethane was added. The reaction mixture was heated to reflux for 2 hours, added to a 1/1 mixture of ether and a saturated aqueous K_2CO_3 solution (200 mL) and stirred for 1 additional h. The organic layer was separated, and the aqueous layer was extracted with ether (2 x 50 mL). The combined organic layers were dried over $MgSO_4$, filtered and concentrated *in vacuo*. The product was purified using column chromatography (SiO_2, EtOAc/pentane 10/1) and subsequent recrystallization from hot ethyl acetate and heptane. Indanone **5.4** was obtained as a white crystalline solid (2.81 g, 13.1 mmol, 22%). ^{1}H NMR (400 MHz,

$CDCl_3$) δ 7.01 (s, 1H), 3.94 (s, 3H), 3.93 (s, 3H), 3.86 (s, 3H), 3.05 – 2.99 (m, 2H), 2.67 – 2.61 (m, 2H); ^{13}C NMR (101 MHz, $CDCl_3$) δ 206.2, 154.5, 150.5, 147.86, 141.8, 132.7, 100.8, 61.3, 60.8, 56.4, 36.4, 22.6; mp: 82 °C; HRMS (ESI): calcd for ($[C_{12}H_{15}O_4+H]^+$): 223.09649, found 223.09619.

3-(2,3-dimethoxyphenyl)acrylic acid (5.5)

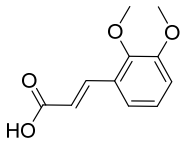

2,3-Dimethoxybenzaldehyde (10.0 g, 60.2 mmol) and malonic acid (12.2 g, 120 mmol) were mixed in pyridine (24 mL) at 50 °C until both were dissolved. Piperidine (0.9 mL) was added and the mixture was heated to 80 °C for 1h, and subsequently at reflux for 3 h. The reaction mixture was then cooled to room temperature and poured on 225 mL of water. Concentrated HCl (28 mL) was added and the mixture was filtered using a glass filter. The residue was washed with water and redissolved in 2 M NaOH (aq.) (250 mL). The solution was filtered, diluted and acidified with concentrated HCl. The product was collected by filtration and washed with water. The residue was dissolved in ethyl acetate, washed with brine, dried over $MgSO_4$ and concentrated *in vacuo*. The product was obtained as a white, fluffy crystalline solid (10.3 g, 49.5 mmol, 82.2%). ^1H NMR (400 MHz, $CDCl_3$) δ 8.10 (d, *J* = 16.1 Hz, 1H), 7.16 (dd, *J* = 7.9, 1.4 Hz, 1H), 7.06 (t, *J* = 8.0 Hz, 1H), 6.95 (dd, *J* = 8.1, 1.4 Hz, 1H), 6.49 (d, *J* = 16.1 Hz, 1H), 3.87 (d, *J* = 1.9 Hz, 6H); ^{13}C NMR (101 MHz, $CDCl_3$) δ 172.3, 153.4, 148.9, 142.0, 128.5, 124.4, 119.7, 118.7, 114.6, 61.6, 56.1; mp: 181-182 °C; HRMS (ESI): calcd for ($[C_{11}H_{12}O_4+H]^+$): 231.06278, found 231.06267.

3-(2,3-dimethoxyphenyl)propanoic acid (5.6)

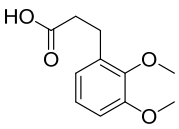

Carboxylic acid **5.5** (10.0 g, 43.3 mmol) was suspended in absolute ethanol (150 mL) in a 2 L three-necked flask fitted with a septum, stopper and a nitrogen line with valve. Ethyl acetate (300 mL) was added until all starting material had dissolved. Pd/C (10 wt. %) (1 g) and 5 drops of acetic acid were added and the flask was purged with nitrogen. The flask was purged with H_2 (g) and the suspension was stirred vigorously at room temperature for 24 h under 1 bar of H_2. After purging the flask with nitrogen, the suspension was poured over a plug of celite, which was washed with ethyl acetate. The combined organic layers were concentrated *in vacuo* and the product was obtained as a white solid (10.0 g, 43.0 mmol, 99%). ^1H NMR (300 MHz, $CDCl_3$) δ 6.97 (t, *J* = 7.9 Hz, 1H), 6.83 – 6.74 (m, 2H), 3.84 (s, 3H), 3.82 (s, 3H), 2.94 (t, *J* = 7.5 Hz, 2H), 2.65 (t, *J* = 7.5 Hz, 2H); ^{13}C NMR (101 MHz, $CDCl_3$) δ 179.1, 153.0, 147.4, 134.2, 124.2, 121.9, 111.1, 60.8, 55.9, 34.8, 25.5; mp: 59 °C; HRMS (ESI): calcd for ($[C_{11}H_{14}O_4+H]^+$): 233.07843, found 233.07823.

4,5-dimethoxy-2,3-dihydro-1*H*-inden-1-one (5.7)

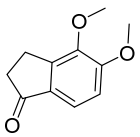

Carboxylic acid **5.6** (3.57 g, 17.0 mmol) and $SOCl_2$ (2.5 mL, 34 mmol) were heated to 80 °C in dry toluene (45 mL) for 1 h. After removal of the solvent *in vacuo*, the crude material was redissolved in toluene and again concentrated *in vacuo*. The crude material was subsequently dissolved in dry DCM (100 mL) and cooled to -78 °C. Aluminium trichloride (2.49 g, 18.7 mmol) was added and the mixture was allowed to heat up to room temperature. The solution was poured on ice after which the water layer was extracted with DCM (3 x 50 mL). The combined organic layers were dried over $MgSO_4$ and concentrated *in vacuo*. The crude material was purified by flash column chromatography (SiO_2, pentane/ethyl acetate 9/1) and ketone **5.7** was obtained as a white crystalline solid (2.57 g, 13.4 mmol, 79%). ^{1}H NMR (400 MHz, $CDCl_3$) δ 7.51 (d, *J* = 8.3 Hz, 1H), 6.95 (d, *J* = 8.4 Hz, 1H), 3.93 (s, 3H), 3.90 (s, 3H), 3.14 – 3.05 (m, 2H), 2.69 – 2.63 (m, 2H); ^{13}C NMR (101 MHz, $CDCl_3$) δ 205.6, 157.6, 147.9, 145.4, 131.1, 120.2, 112.3, 60.3, 56.2, 36.4, 22.5; mp: 73-74 °C; HRMS (ESI): calcd for ($[C_{11}H_{13}O_3$+H]$^+$): 193.08592, found 193.08564.

4-hydroxy-5-methoxy-2,3-dihydro-1*H*-inden-1-one (5.8)

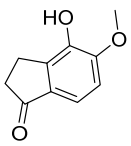

Aluminium trichloride (3.04 g, 22.8 mmol) was suspended in DCM (10 mL) on ice. Trimethylamine hydrochloride (1.09 g, 11.4 mmol) was added and the mixture was stirred and warmed up to room temperature over 3h. Ketone **5.7** (626 mg, 3.26 mmol) was dissolved in DCM (40 mL) and the ionic liquid was added dropwise to the solution. The reaction mixture was heated at reflux for 24 h and subsequently poured into 50 mL 1 M HCl (aq.). The aqueous phase was extracted with chloroform (4 x 50 mL) and the combined organic layers were washed with brine, dried over $MgSO_4$ and concentrated *in vacuo*. Both regioisomers were produced, but by ^{1}H NMR analysis, the desired product was calculated to have been obtained in 84% selectivity, in 70% overall yield. The desired regioisomer could be crystallized from hot ethyl acetate and was obtained as a clear colourless crystalline solid (317 mg, 1.78 mmol, 55%). ^{1}H NMR (400 MHz, $CDCl_3$) δ 7.34 (d, *J* = 8.3 Hz, 1H), 6.91 (d, *J* = 8.3 Hz, 1H), 5.75 (s, 1H), 3.95 (s, 3H), 3.09 – 3.01 (m, 2H), 2.71 – 2.63 (m, 2H); ^{13}C NMR (101 MHz, $CDCl_3$) δ 206.2, 151.1, 142.4, 140.7, 131.7, 116.4, 110.7, 56.7, 36.8, 22.1; mp: 192-193 °C; HRMS (ESI): calcd for ($[C_{10}H_{11}O_3$+H]$^+$): 179.07027, found 179.07018.

4-((tert-butyldimethylsilyl)oxy)-5-methoxy-2,3-dihydro-1*H*-inden-1-one (5.9)

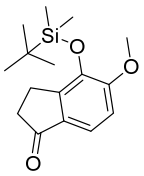

Ketone **5.8** (614 mg, 3.45 mmol), 4-DMAP (465 mg, 3.80 mmol) and *tert*-butyldimethylsilyl chloride (2.87 g, 18.9 mmol) were mixed in dry DCM (20 mL) and the mixture was stirred at room temperature under a nitrogen atmosphere. Conversion was followed by TLC and after 48 h the reaction was quenched by adding 30 mL of NH_4Cl (aq. sat.). The aqueous layer was extracted with DCM (3 x 25 mL) and the combined organic layers were dried over $MgSO_4$ and concentrated *in vacuo*. The crude material was purified by flash column chromatography (SiO_2, pentane/ethyl acetate 19/1) and TBS-protected ketone **5.9** was obtained as a white crystalline solid (868 mg, 2.97 mmol, 87%). ^{1}H NMR (400 MHz, $CDCl_3$) δ 7.38 (d, *J* = 8.3 Hz, 1H), 6.90 (d, *J* = 8.3 Hz, 1H), 3.86 (s, 3H), 3.05 – 2.97 (m, 2H), 2.67 – 2.59 (m, 2H), 1.01 (s, 9H), 0.17 (s, 6H); ^{13}C NMR (101 MHz, $CDCl_3$) δ 206.2, 155.4, 146.7, 141.8, 131.5, 117.7, 111.8, 55.7, 36.7, 26.1, 23.3, 18.9, -3.8; mp = 122 °C; HRMS (ESI): calcd for ($[C_{16}H_{25}O_3Si+H]^+$): 293.15675, found 293.15689.

(*E*)-tert-butyldimethyl((4',5,5',6'-tetramethoxy-2,2',3,3'-tetrahydro-[1,1'-biindenylidene]-4-yl)oxy)silane (*trans*-5.10)

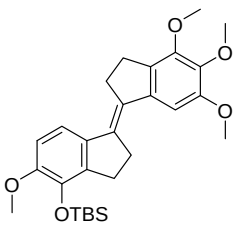

Zn (894 mg, 13.7 mmol) was suspended in 10 mL dry THF in a 25 mL two-necked flask, equipped with a rubber septum and a reflux condenser, under a nitrogen atmosphere. $TiCl_4$ (743 µL, 1.29 g, 6.84 mmol) was added dropwise to the stirred suspension and the mixture was heated to reflux for 2h. Ketone **5.4** (380 mg, 1.71 mmol) and ketone **5.9** (500 mg, 1.71 mmol) were dissolved together in 15 mL of dry THF. The solution was added to the reaction mixture and subsequently heated at reflux for 18 h. The reaction mixture was cooled down to room temperature and filtered over a plug of celite, which was subsequently washed with ethyl acetate. The combined organic layers were washed with brine (1 x 50 mL), dried over $MgSO_4$ and concentrated *in vacuo*. The crude product was purified by flash column chromatography (SiO_2, pentane/EtOAc 95:5). The product was obtained as the pure *trans* isomer, as identified by NOESY-NMR (349 mg, 0.72 mmol, 42%). ^{1}H NMR (400 MHz, $CDCl_3$) δ 7.14 (d, *J* = 8.4 Hz, 1H), 6.92 (s, 1H), 6.78 (d, J = 8.4 Hz, 1H), 3.90 (s, 3H), 3.89 (s, 3H), 3.88 (s, 3H), 3.81 (s, 3H), 3.15 – 2.98 (m, 8H), 1.00 (s, 9H), 0.17 (s, 6H); ^{13}C NMR (101 MHz, $CDCl_3$) δ 153.0, 149.8, 149.7, 141.3, 141.1, 139.5, 138.6, 137.6, 134.6, 133.6, 132.0, 117.6, 110.6, 104.0, 61.3, 60.6, 56.5, 55.6, 32.2, 32.1, 28.8, 27.8, 26.2, 18.9, -3.9; mp: 130 °C; HRMS (APCI): calcd for ($[C_{28}H_{38}O_5Si+H]^+$): 483.25613, found 483.25514.

(*Z*)-tert-butyldimethyl((4',5,5',6'-tetramethoxy-2,2',3,3'-tetrahydro-[1,1'-biindenylidene]-4-yl)oxy)silane (*cis*-5.10)

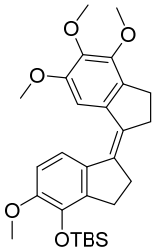

Trans colchicine analogue **5.10** was dissolved in dry acetonitrile. The solution was purged with Ar and irradiated with 312 nm UV light until after 3 h the PSS was reached. ^{1}H NMR analysis showed 55% isomerization to the *cis* isomer. The isomers were separated by flash column chromatography (SiO_2, pentane/EtOAc 96:4) and the product was isolated as a brown oil. NOESY-NMR confirmed formation of the *cis* isomer. ^{1}H NMR (400 MHz, CD_3CN) δ 7.64 (d, *J* = 8.4 Hz, 1H), 7.42 (s, 1H), 6.81 (d, *J* = 8.5 Hz, 1H), 3.85 (s, 3H), 3.80 (app s, 6H), 3.78 (d, *J* = 1.1 Hz, 3H), 2.89 (m, 4H), 2.76 (m, 4H), 1.01 (s, 9H), 0.18 (s, 6H). No ^{13}C spectrum was recorded.

(*E*)-4',5,5',6'-tetramethoxy-2,2',3,3'-tetrahydro-[1,1'-biindenylidene]-4-ol (*trans*-5.3)

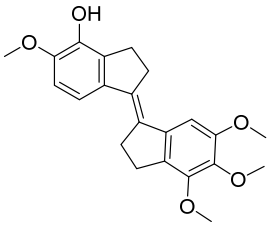

Stiff-stilbene *trans*-**5.10** (104 mg, 0.216 mmol) was dissolved in THF (10 mL) and cooled in an ice bath. 1M TBAF in THF (430 µL, 0.430 mmol) was added dropwise and the stirred solution was taken out of the ice bath. Conversion was monitored by TLC and the reaction was quenched with water (10 mL) after 1 h. The aqueous layer was extracted with ethyl acetate (3 x 10 mL). The combined organic layers were dried over $MgSO_4$ and concentrated *in vacuo*. The crude material was purified by column chromatography (SiO_2, pentane/EtOAc 4:1). *Trans*-stilbene **5.3** was obtained as a yellow solid (60.0 mg, 0.163 mmol, 76%). ^{1}H NMR (400 MHz, $CDCl_3$) δ 7.10 (d, *J* = 8.4 Hz, 1H), 6.95 (s, 1H), 6.81 (d, *J* = 8.4 Hz, 1H), 5.63 (s, 1H), 3.93 (app. s, 6H), 3.92 (s, 3H), 3.90 (s, 3H), 3.25 – 3.13 (m, 2H), 3.14 – 3.01 (m, 6H); ^{13}C NMR (101 MHz, $CDCl_3$) δ 152.3, 149.8, 145.8, 141.8, 141.0, 139.4, 138.1, 134.2, 134.2, 132.4, 132.1, 116.2, 109.5, 104.1, 61.3, 60.6, 56.6, 56.5, 32.2, 32.2, 27.8, 27.4; mp: 138 °C; HRMS (APCI): calcd for ($[C_{22}H_{24}O_5+H]^+$): 369.16965, found 369.16956.

5.6 References

1 J. E. Fenn, R. Udelsman, *J. Am. Coll. Surg.* **2011**, *212*, 413–417.
2 V. Malhotra, M. C. Perry, *Cancer Biol. Ther.* **2003**, *2*, S2.
3 V. S. Periyakoil, E. Neri, A. Fong, H. Kraemer, *PLoS One* **2014**, *9*, e98246.
4 R. Weissleder, V. Ntziachristos, *Nat. Med.* **2003**, *9*, 123–128.
5 G. Mayer, A. Heckel, *Angew. Chem. Int. Ed.* **2006**, *45*, 4900–4921.
6 W. A. Velema, J. P. van der Berg, M. J. Hansen, W. Szymanski, A. J. M. Driessen, B. L. Feringa, *Nat. Chem.* **2013**, *5*, 924–928.
7 R. Ferreira, J. R. Nilsson, C. Solano, J. Andréasson, M. Grøtli, *Sci. Rep.* **2015**, *5*, 9765.
8 L. Chen, Y. Zhu, D. Yang, R. Zou, J. Wu, H. Tian, *Sci. Rep.* **2014**, *4*, 6860.
9 W. A. Velema, W. Szymanski, B. L. Feringa, *J. Am. Chem. Soc.* **2014**, *136*, 2178–2191.
10 M. M. Lerch, M. J. Hansen, G. M. van Dam, W. Szymanski, B. L. Feringa, *Angew. Chem. Int. Ed.*, **2016**, *55*, 10978–10999.

11 F. Reeßing, W. Szymanski, *Curr. Med. Chem.* **2016**, *23*, asap.
12 J. Broichhagen, D. Trauner, *Curr. Op. Chem. Biol.* **2014**, *21*, 121–127.
13 J. Broichhagen, J. A. Frank, D. Trauner, *Acc. Chem. Res.* **2015**, *48*, 1947–1960.
14 D. Wang, S. J. Lippard, *Nat. Rev. Drug Deliv.* **2005**, *4*, 307–320.
15 M. Peyrone, *Justus Liebigs Ann. Chem.* **1844**, *51*, 1–29.
16 B. Rosenberg, L. van Camp, J. E. Trosko, V. H. Mansour, *Nature* **1969**, *222*, 385–386.
17 J. J. Roberts, F. Friedlos, *Cancer Res.* **1986**, *47*, 31–36.
18 S. E. Sherman, S. J. Lippard, *Chem. Rev.* **1987**, *87*, 1153–1181.
19 R. Ciccarelli, M. Solomon, *Biochemistry* **1985**, *24*, 7533–7540.
20 A. Presa, R. F. Brissos, A. B. Caballero, I. Borilovic, L. Korrodi-Gregório, R. Pérez-Tomás, O. Roubeau, P. Gamez, *Angew. Chem. Int. Ed.* **2015**, *15*, 4644–4648.
21 J. Wang, B. L. Feringa, *Science* **2011**, *331*, 1429–1432.
22 I. N. Stepanenko, B. Cebrián-Losantos, V. B. Arion, A. A. Krokhin, A. A. Nazarov, B. K. Keppler, *Eur. J. Inorg. Chem.* **2007**, *2*, 400–411.
23 D. Devlitsarov, *Optical Control of Bioactive Molecules*, MSc Research Project Report, University of Groningen, 2015.
24 M. D. Hall, K. A. Telma, K. E. Chang, T. D. Lee, J. P. Madigan, J. R. Lloyd, I. S. Goldlust, J. D. Hoeschele, M. M. Gottesman, *Cancer Res.* **2014**, *74*, 3913–3922.
25 B. Bhattacharyya, D. Panda, S. Gupta, M. Banerjee, *Med. Res. Rev.* **2008**, *28*, 155–183.
26 G. R. Pettit, S. B. Singh, E. Hamel, C. M. Lin, D. S. Alberts, D. Garcia-Kendal, *Experientia* **1989**, *45*, 209–211.
27 G. C. Tron, T. Pirali, G. Sorba, F. Pagliai, S. Busacca, A. A. Genazzani, *J. Med. Chem.* **2006**, *49*, 3033–3044.
28 J. Griggs, R. Hesketh, G. A. Smith, K. M. Brindle, J. C. Metcalfe, G. A. Thomas, E. D. Williams, *Br. J. Cancer* **2001**, *84*, 832–835.
29 G. R. Pettit, M. R. Rhodes, D. L. Herald, E. Hamel, J. M. Schmidt, R. K. Pettit, *J. Med. Chem.* **2005**, *48*, 4087–4089.
30 M. Borowiak, W. Nahaboo, M. Reynders, K. Nekolla, P. Jalinot, J. Hasserodt, M. Rehberg, M. Delattre, S. Zahler, A. Vollmar, D. Trauner, O. Thorn-Seshold, *Cell* **2015**, *162*, 403–411.
31 A. J. Engdahl, E. A. Torres, S. E. Lock, T. B. Engdahl, P. S. Mertz, C. N. Streu, *Org. Lett.* **2015**, *17*, 4546–4549.
32 J. E. Sheldon, M. M. Dcona, C. E. Lyons, J. C. Hackett, M. C. T. Hartman, *Org. Biomol. Chem.* **2015**, *14*, 40–49.
33 A. Meister, M. E. Anderson, *Annu. Rev. Biochem.* **1983**, *52*, 711–760.
34 M. A. Brown, S. C. De Vito, *Crit. Rev. Environ. Sci. Technol.* **1993**, *23*, 249–324.
35 A. A. Beharry, L. Wong, V. Tropepe, G. A. Woolley, *Angew. Chem. Int. Ed.* **2011**, *50*, 1325–1327.
36 F. B. Mallory, C. W. Mallory, *Photocyclization of Stilbenes and Related Molecules*, in *Organic Reactions Vol. 30*, ed. W. G. Dauben *et al*, John Wiley & Sons Inc., Hoboken, NJ, 1984.
37 M. Oelgemöller, R. Frank, P. Lemmen, D. Lenoir, J. Lex, Y. Inoue, *Tetrahedron* **2012**, *68*, 4048–4056.
38 G. Nenajdenko, I. L. Baraznenok, S. Baler, *Tetrahedron* **1996**, *52*, 12993–13006.
39 G. J. Kemperman, T. A. Roeters, P. W. Hilberink, *Eur. J. Inorg. Chem.* **2003**, *9*, 1681–1686.